2008 IEEE/RSJ International Conference on Intelligent Robots and Systems
Acropolis Convention Center
Nice, France, Sept, 22-26, 2008

High-speed Throwing Motion Based on Kinetic Chain Approach

Taku Senoo, Akio Namiki and Masatoshi Ishikawa

***Abstract*— In this paper the robotic throwing task is considered with the goal of achieving high-speed dynamic manipulation. We propose a kinetic chain approach for swing motion focused on torque transmission. In addition the release method using a robotic hand is analyzed for ball control. Experimental results are shown in which a high-speed manipulator throws a ball toward a target.**

I. INTRODUCTION

Recently highly efficient robotic components have lead to various robot improvements such as multi-fingered hands and biped walking robots that have more extendibility than previously. In terms of motor performance, however, there are few robots equipped with quickness.

Fast movement for robot systems provides not only improvement in operating efficiency. And high-speed robotic control has great potential to enable performance of new skills and new applications. For example some previous studies have been reported such as dynamic regrasping [1] and high-speed batting [2]. However, there is little previous work where high-speed hand-arm coordination manipulation is achieved.

In this paper we report on experiments on the robotic throwing motion using a hand-arm system as shown in Fig.1. First a strategy for arm control is proposed based on the "kinetic chain" which is observed in human throwing motion. This strategy produces efficient high-speed motion using base functions of two types derived from approximate dynamics. Next the method of release control with a robotic hand is represented based on analysis related to contact state during a fast swing. The release method employs features so that the apparent force, almost all of which is generated by high-speed motion, plays a roll in robust control of the ball direction. Finally our high-speed manipulation system is described and experimental results are shown.

II. SPEEDING UP SWING MOTION

In this section we extract a motional framework for producing high-speed movement based on human swing motion. The proposed swing model can be adapted to any two-link robot arm with rotational joints. It is possible to convert model-based motion into motion corresponding to actual equipment even if there are differences in kinematics between them.

T. Senoo and M. Ishikawa are with Dept. of Creative Informatics, Graduate School of Information Science and Technology, University of Tokyo, 7-3-1 Hongo, Bunkyo-ku, Tokyo 113-8656, Japan. Taku_Seno@ipc.i.u-tokyo.ac.jp

A. Namiki is with Dept. of Mechanical Engineering, Graduate School of Engineering, Chiba University, 1-33 Yayoi-cho Inage-ku Chiba-shi, Chiba 263-8522, Japan. namiki@faculty.chiba-u.jp

A. Human Swing Motion

We see human motion at tremendous speeds in sports. For example the speed of an elbow joint in the throwing motion can be up to 40 [rad/s] [3]. However the observed torque of triceps brachii, which generates the elbow motion, is remarkably low considering the speed. Focusing on the speed or power in distal upper extremity, their values are dramatically increased just before release time. This is because a human has a mechanism to explosively radiate kinetic energy accumulated from the early stages of a swing motion. This mechanism is called "kinetic chain" and it achieves high-speed swing motion efficiently. Two factors are particularly important.

One is two-dimensional kinetic chain, which means power transmission [4]. This motion has characteristics so that the peak of the velocity waveform is continuously moved from the body trunk to the distal part.

The other is three-dimensional kinetic chain. This means the effect of motion generated by rotation about axes, the directions of which are different from each other like gyro [5].

B. Swing Model and Its Dynamics

We propose a swing model to constitute the framework of kinetic chain. Figure 2 shows the swing model composed of the upper arm and the lower arm. This model has a total of 3-DOF and consists of two revolution joints (q_1, q_3) at the shoulder and the elbow respectively and a coupled bending joint (q_2) to keep the lower arm horizontal. This model corresponds to the above two factors of kinetic chain as described below.

- Axis-1 and axis-3 are parallel. The state with the elbow in extension $(q_2 = \pi/2)$ results in two-dimensional planar model.
- Axis-2 is perpendicular to other axes. The rotation about axis-2 produces 3D interferential action.

Next we derive the equation of motion. To simplify the problem, we ignore the moment of inertia. Gravity is also

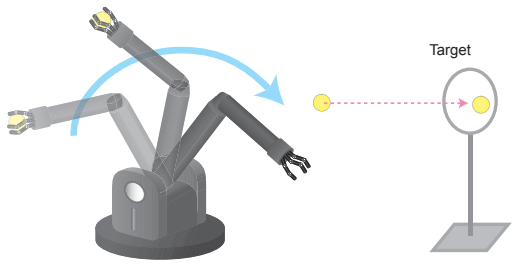

Fig. 1. Throwing motion using a hand-arm system

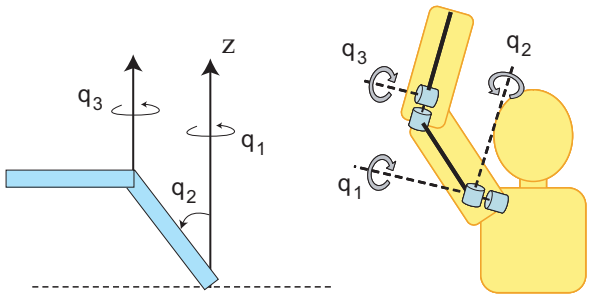

Fig. 2. Swing Model

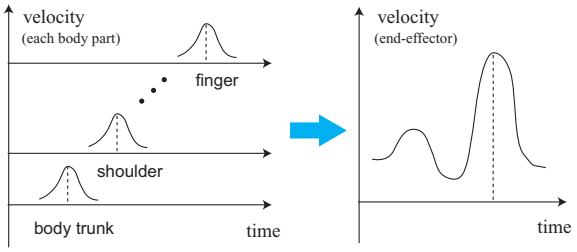

Fig. 3. Superposition of base functions

ignored to clarify the effect of interaction between joints. Because of this assumption the dynamics does not depend on the choice of coordinate system, so the model can accommodate various types of throwing such as overhand pitch, sidearm pitch and underarm pitch.

The torque $\boldsymbol{\tau}$ is computed as

$$\boldsymbol{\tau} = \boldsymbol{M}(\boldsymbol{q})\ddot{\boldsymbol{q}} + \boldsymbol{h}(\boldsymbol{q}, \dot{\boldsymbol{q}}) \ , \tag{1}$$

where $\boldsymbol{M}(\boldsymbol{q})$ is the inertia matrix, $\boldsymbol{h}(\boldsymbol{q}, \dot{\boldsymbol{q}})$ is the coriolis and centrifugal force term. Those elements are represented as

$$\begin{aligned} M_{22} &= J_1 + 4J_2C_3^2 + 4A_{12}S_2C_3 + B_2 \ , \\ M_{23} &= M_{32} = -A_{12}C_2S_3 \ , \ M_{33} = J_2 \ , \\ h_2 &= -\frac{1}{2}(J_1 + B_2)\sin(2q_2)\dot{q}_1^2 - 4J_2\sin(2q_3)\dot{q}_2\dot{q}_3 \\ &\quad - A_{12}C_2C_3(2\dot{q}_1\dot{q}_3 + \dot{q}_3^2 + 2\dot{q}_2^2 + \dot{q}_1^2) - 4A_{12}S_2S_3\dot{q}_2\dot{q}_3 \ , \\ h_3 &= 2A_{12}C_2C_3\dot{q}_1\dot{q}_2 + A_{12}S_2S_3(\dot{q}_2^2 + \dot{q}_1^2) + 2J_2\sin(2q_3)\dot{q}_2^2 \ , \end{aligned} \tag{2}$$

where $S_i \equiv \sin q_i$ and $C_i \equiv \cos q_i$. Other constant parameters are defined as follows;

$$\begin{aligned} J_1 = m_1L_{1g}^2 \ , \ J_2 = m_2L_{2g}^2 \ , \\ A_{12} = m_2L_1L_{2g} \ , \ B_2 = m_2L_1^2 \ , \end{aligned} \tag{3}$$

where m_i, L_i, L_{ig} corresponding to i-th link means the mass, the entire length and the length to center of gravity respectively. We assume that the parameter including m_1 is larger than other parameters because the upper arm is generally heavier than the lower arm;

$$J_1 \gg J_2 \, , \, A_{12} \, , \, B_2 \ . \tag{4}$$

C. Decomposition into Base Functions

The essence of the kinetic chain approach is efficient transmission of power from body trunk to distal part. Because in this model joint-1 represents the source of power, the motion driven by the interaction is desirable behavior for joint-2 and joint-3. Therefore we set $\boldsymbol{\tau} \simeq \boldsymbol{0}$ except for joint-1;

$$\boldsymbol{M}(\boldsymbol{q})\ddot{\boldsymbol{q}} + \boldsymbol{h}(\boldsymbol{q}, \dot{\boldsymbol{q}}) \simeq \boldsymbol{0} \ . \tag{5}$$

Suppose that joint-1 can output higher power than the other joints and achieve steady state high-speed rotation instantaneously;

$$\begin{aligned} \dot{q}_1 \gg \dot{q}_i \quad (i \neq 1) \ , \\ \dot{q}_1 = \text{constant}, \quad \ddot{q}_1 = 0 \ . \end{aligned} \tag{6}$$

1) Motion of Joint-2: To obtain motion in joint-2, the vector $\ddot{\boldsymbol{q}} = [0, \ddot{q}_2, 0]^T$ is substituted for Eq.(5) thereby setting joint-3 in continuous uniform motion $\ddot{q}_3 = 0$. The dynamics of joint-2 is approximated using the above assumption;

$$(J_1 + B_2)\ddot{q}_2 - \frac{1}{2}(J_1 + B_2)\dot{q}_1{}^2\sin(2q_2) \simeq 0 \ . \tag{7}$$

If we express $\sin 2q_2 \simeq 2q_2$ using the first-order approximation of the Taylor series, this equation becomes a second order differential equation for q_2. The solution is

$$q_2 \simeq \alpha_2 \exp(\omega_2 t + \phi_2) \ , \tag{8}$$

where ω_2, ϕ_2 and α_2 are frequency, phase, and amplitude respectively. That is an exp-type base function representing a three-dimensional interaction of inertia force.

2) Motion of Joint-3: To obtain motion of joint-3, the vector $\ddot{\boldsymbol{q}} = [0, 0, \ddot{q}_3]^T$ is substituted for Eq.(5) thereby setting joint-2 in continuous uniform motion $\ddot{q}_2 = 0$. The dynamics of joint-3 is approximated using the above assumption;

$$J_2\ddot{q}_3 + A_{12}\dot{q}_1{}^2S_2S_3 \simeq 0 \ . \tag{9}$$

If we express $S_3 \simeq q_3$ using the first-order approximation of the Taylor series and consider S_2 as constant, this equation becomes a second order differential equation for q_3. The solution is

$$q_3 \simeq \alpha_3 \sin(\omega_3 t + \phi_3) \ , \tag{10}$$

where ω_3, ϕ_3 and α_3 are frequency, phase, and amplitude respectively. That is a sin-type base function representing the two-dimensional kinetic chain.

Although we can calculate the frequency parameters $\boldsymbol{\omega}$ by Eqs.(7) and (9), these equations are rough approximations of the dynamics. Therefore we calculate the frequency parameters as well as other unknown parameters $\boldsymbol{\phi}, \boldsymbol{\alpha}$ in the next section. In addition we also set the trajectory of joint-1 as a sin-type base function. We express parameters concerning the base function as

$$\boldsymbol{\xi}^T = \begin{bmatrix} \boldsymbol{\omega}^T & \boldsymbol{\phi}^T & \boldsymbol{\alpha}^T \end{bmatrix} \ . \tag{11}$$

The constant term $\boldsymbol{c}$ is added to the base functions to ensure continuity of motion. Then the trajectory of joint angles is

$$\boldsymbol{q}(\boldsymbol{\xi}, t) = \begin{bmatrix} \alpha_1 \sin(\omega_1 t + \phi_1) + c_1 \\ \alpha_2 \exp(\omega_2 t + \phi_2) + c_2 \\ \alpha_3 \sin(\omega_3 t + \phi_3) + c_3 \end{bmatrix} \ . \tag{12}$$

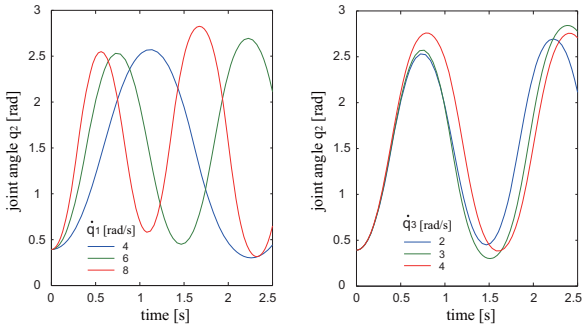

Fig. 4. Change of joint angle q_2 with respect to angular velocity

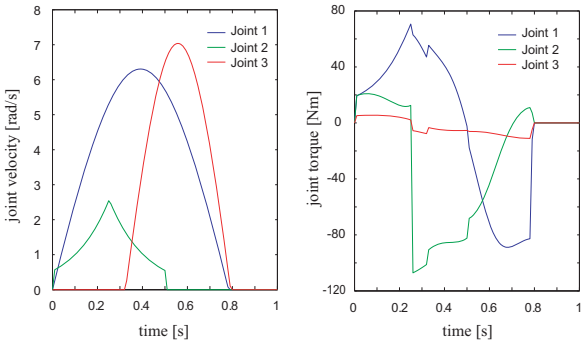

Fig. 5. Time response of joint velocity and joint torque

The trajectory of velocity and acceleration is the same type of function. Because the behavior of exp-type functions is monotonically increasing (or decreasing), we change the sign of ω_2 at a certain time to decelerate swing motion.

D. Superposition of Base Functions

We synthesize the decomposed base functions so that the speed of the end-effector is increased as shown in Fig.3. The velocity of the end-effector $\dot{\boldsymbol{r}}_E$ is represented as a function $\boldsymbol{f}$ of base function parameters and the time variable:

$$\dot{\boldsymbol{r}}_E = \boldsymbol{f}(\boldsymbol{\xi}, t) \ . \tag{13}$$

In each joint the start time t_{si} and the termination time t_{ei} of the swing are defined by Eq.(12) so that the joint velocity equals zero;

$$t_{si} = \frac{-\phi_i - \pi/2}{\omega_i} \ , \quad t_{ei} = \frac{-\phi_i + \pi/2}{\omega_i} \ . \tag{14}$$

Although the joint velocity for exp-type functions does not go to zero exactly, the time is defined in a similar way.

Under the kinematics constraint and dynamics constraint, the parameter $\boldsymbol{\xi}$ is set so as to maximize the following evaluation function:

$$\max_{\boldsymbol{\xi},\, t} \dot{\boldsymbol{r}}_E^T K_r \dot{\boldsymbol{r}}_E \tag{15}$$

subject to

$$\boldsymbol{q}_{\min} \le \boldsymbol{q} \le \boldsymbol{q}_{\max} \ , \ \dot{\boldsymbol{q}}_{\min} \le \dot{\boldsymbol{q}} \le \dot{\boldsymbol{q}}_{\max} \ ,$$
$$\boldsymbol{\tau}_{\min} \le \boldsymbol{\tau} \le \boldsymbol{\tau}_{\max} \ , \ t_s \le t \le t_e \ ,$$

where K_r is a positive definite matrix, $t_s = \min t_{si}$, $t_e = \max t_{ei}$, and a suffix $\max$ or $\min$ means the maximum and minimum of the variable respectively. This computation is equivalent to maximizing the translational kinetic energy of the end-effector motion when $K_r = \mathrm{diag}[\frac{1}{2}m_e, \frac{1}{2}m_e, \frac{1}{2}m_e]$, where m_e is the effective mass of the end-effector.

E. Simulation

For optimization, we set the constraint using data from the barrett arm, which is described in section IV-A. The SQP method was used as the optimized calculation.

The change in joint angle q_2 with respect to joint velocities $\dot{q_1}, \dot{q_3}$ is shown in Fig.4. The left figure shows the case where $\dot{q_1}$ is constant and $\dot{q_3}$ varies. The right figure shows the reverse case. In those figures the frequency of joint-2 depends not on $\dot{q_3}$ but on $\dot{q_1}$. Because this result corresponds to the behavior of Eq.(7), it proves the validity of the approximation of the dynamics. In addition it turns out that joint-2 oscillates around $q_2 = \pi/2$. This means that the apparent force acts so that it extends the arm as in a human throwing motion. The oscillation is attributable to the mechanism of rotational joints.

Figure 5 represents the time response of joint velocity and torque. In the left figure it turns out that the trajectories of both joint-1 and joint-3 are expressed by a sin-type function and the trajectory of joint-2 is expressed by an exp-type function. In the sin-type trajectories we can observe the transition of peak time as a typical characteristic of planar kinetic chain. The torque of joint-1 increases sharply from the start time $t = 0$. On the other hand the torque of joint-2 gradually goes to zero although joint-2 also gets into motion. This is as expected for an exp-type function. At $t = 0.26$ the torque of joint-2 decreases dramatically. This is because the motion of joint-2 switches to decreasing speed due to the constraint of joint angles against the force heading to $q_2 = \pi/2$. Moreover joint-3 moves fast despite the low torque of joint-3 during its motion. This is as expected for a sin-type function.

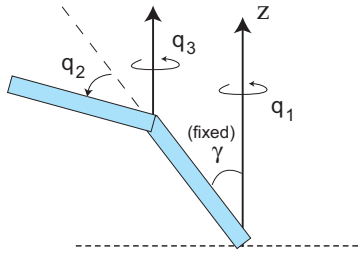

Fig. 6. Analogous Swing Model

F. Analogous Swing Model

Let's consider the analogous swing model shown in Fig.6. The difference between the two models is the placement of joint-2. The angle γ between axis-1 and the upper arm is fixed. We calculate the dynamics of this model and simulate swing motion in a similar way.

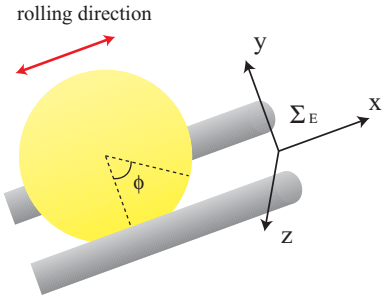

Fig. 7. Contact model between a hand and a ball

The dynamics of joint-2 is approximated as

$$J_2\ddot{q}_2 - \frac{1}{2}J_2\dot{q}_1^2\sin(2(\gamma+q_2)) \simeq 0\ . \tag{16}$$

This equation is solved with an exp-type function. The motion of joint-2 oscillates around $q_2+\gamma = \pi/2$. The dynamics of joint-3 is approximated as

$$J_2 S_{\gamma 2}\ddot{q}_3 + A_{12}\dot{q}_1^2 S_\gamma S_3 \simeq 0\ . \tag{17}$$

This equation is solved with a sin-type function.

The analogy between the two models shows the following behavior of high-speed swing motion. The rotations about parallel axes produce a planar sin-type kinetic chain. Moreover rotation about the axis which is perpendicular to the parallel axes produces an exp-type kinetic chain. This motion oscillates around the plane that is perpendicular to the sin-type axes.

We adopt the latter model in the experiment for the following reasons. First, the speed is limited to some extent in the former model because of the constraint of joint angle q_2. Second, the latter model requires less compensating torque for gravity than the former one.

III. CONTROL OF A THROWN BALL

In this section we analyze the model of the contact state between a hand and a ball. Next the method for ball control is described.

A. Modeling of Contact State

Suppose that a hand and a ball are both rigid bodies. The equation of ball motion in the coordinate Σ_E moving in translational acceleration $\boldsymbol{\alpha}_0$ and angular velocity $\boldsymbol{\omega}_0$ against standard coordinate Σ_0 is expressed as

$$\begin{aligned} m\ddot{\boldsymbol{r}}' =& \boldsymbol{F}' + \boldsymbol{g}' - m(\boldsymbol{\alpha}_0' + \dot{\boldsymbol{\omega}}_0' \times \boldsymbol{r}') \\ &+2m\dot{\boldsymbol{r}}' \times \boldsymbol{\omega}_0' + m(\boldsymbol{\omega}_0' \times \boldsymbol{r}') \times \boldsymbol{\omega}_0'\ , \end{aligned} \tag{18}$$

where m is mass of the ball, $\boldsymbol{r}$ is ball position, $\boldsymbol{F}$ is contact force, $\boldsymbol{g}$ is gravity force, and a suffix $'$ means that the variable is expressed in the coordinate Σ_E. The third term is the inertia force due to accelerated motion, the fourth term is the Coriolis force, and the fifth term is the centrifugal force. Since the throwing motion includes three dimensional fast rotatory motion, Eq.(18) contains the considerable effect of the apparent force peculiar to a non-inertial system.

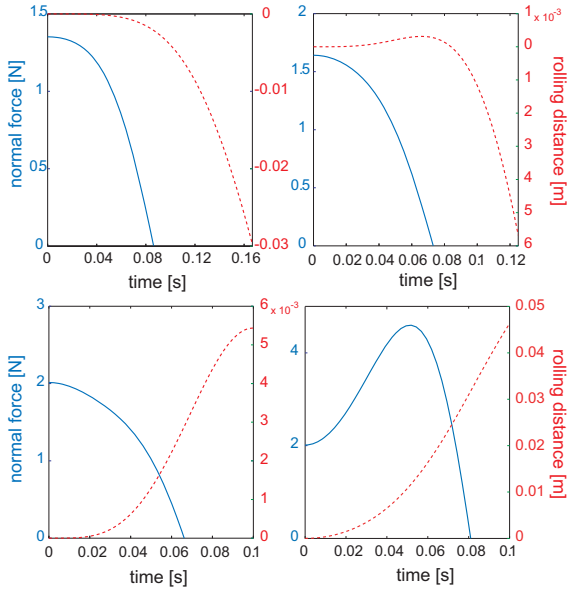

Fig. 8. Relation between normal force and rolling distance

The motion of the hand is set to throw a ball by following three steps.

(i) The hand grasps the ball with three fingers so as not to drop it until a given time.
(ii) The contact state is switched to two-finger contact by releasing one finger at a certain time.
(iii) The two fingers move in the same way and release the ball while the ball rolls along the fingers.

Suppose that the x-axis is set along the two fingers for release, the y-axis is perpendicular to the plane of the two fingers, and the z-axis is set so that the three axes constitute orthogonal coordinates as shown in Fig.7. The condition where the ball with radius a and moment of inertia $I = \frac{2}{5}ma^2$ rolls at angles ϕ without sliding is represented as

$$I\ddot{\phi} = aF_x', \qquad x' = a\phi\ . \tag{19}$$

Since the ball cannot be moved in the y-axis and z-axis until release time, the following conditions are satisfied:

$$y' = \dot{y}' = \ddot{y}' = 0, \qquad z' = \dot{z}' = \ddot{z}' = 0\ . \tag{20}$$

The dynamics of rolling motion is calculated as follows when Eqs.(19) and (20) are substituted for Eq.(18):

$$\ddot{x}' = \frac{5}{7}\left\{-\alpha_{0x}' + g_x' + ({\omega_{0y}'}^2 + {\omega_{0z}'}^2)x'\right\}\ . \tag{21}$$

Similarly, the normal force F_y' is computed as

$$F_y' = m\left\{\alpha_{0y}' - g_y' + 2\omega_{0z}'\dot{x}' + (\dot{\omega}_{0z}' + {\omega_{0x}'}^2)x'\right\}\ . \tag{22}$$

The ball is released from the fingers when the normal force is reduced to zero or less. Then we analyzed the relation between the normal force and the motion of rolling.

Figure 8 shows the rolling distance and the normal force under varying conditions. Depending on the conditions of the

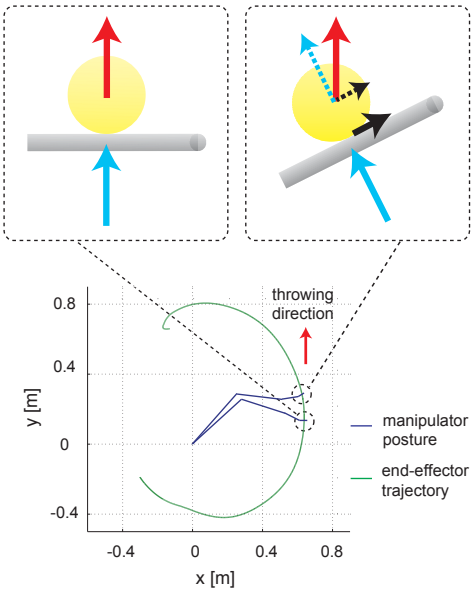

Fig. 9. Rolling effect for control of throwing direction

acceleration and the posture of the manipulator, the ball can roll in either the positive or negative direction, or the hand sometimes releases the ball without the effect of a normal force as soon as the grasping finger is released from the ball. The faster the manipulator moves, the longer generally the rolling distance is. However the rolling distance cannot be dramatically increased. It is only a few centimeters. This is because the motion time becomes short until release of the ball, while fast motion brings fast speed of rolling. Therefore we assume that the ball is released before it rolls to the fingertip.

B. Released Ball Motion

The velocity of the ball expressed in standard coordinates is calculated as follows:

$$\boldsymbol{v} = \boldsymbol{v}_0 + R\dot{\boldsymbol{r}}' + \boldsymbol{\omega} \times R\boldsymbol{r}' \ , \tag{23}$$

where $\boldsymbol{v}_0$ is translational velocity of the end-effector, and R is a rotation matrix from Σ_0 to Σ_E. If the rolling distance is short, the above equation can be approximated as $\boldsymbol{v} \simeq \boldsymbol{v}_0 + R\dot{\boldsymbol{r}}'$. That is, throwing direction depends mainly on the translational velocity of the end-effector and rolling velocity of the ball.

C. Strategy for Ball Control

Based on the above results, two elements are important to ball control. One is control of release timing and the other is control of the direction of release. These two elements are greatly affected by the translational acceleration and the translational velocity respectively. However it is difficult to control these variables in parallel with high accuracy. In addition it is difficult to positively apply the rolling motion to directional control. Therefore we propose a strategy for ball control in which the rolling motion acts secondarily to maintain the throwing direction.

(a) Arm kinematics (b) Hand-Arm system

Fig. 10. High-speed manipulator system

1) Release Timing: We control the hand so that release of grasping finger and release of the ball are performed at the same time. Because both rolling distant and rolling velocity are zero at release time, the normal force is represented as $F'_y = m(\alpha'_{0y} - g'_y)$ by Eq.(22). Therefore the grasping finger is controlled to release the ball when the following condition is satisfied;

$$\alpha'_{0y} < g'_y \ . \tag{24}$$

2) Release Direction: We control the hand so that the ball is released in the tangential direction of the end-effector trajectory at release point. This condition of control is represented as

$$v'_{0x} = 0, \qquad \alpha'_{0x} < 0 \ . \tag{25}$$

The rolling acceleration near release point is expressed as $\ddot{x}' = \frac{5}{7}(-\alpha'_{0x} + g'_x)$ by Eq.(21). Therefore the ball rolls toward distal direction of the finger if $\alpha'_{0x} < g'_x$. On the other hand the velocity of the finger just after release is $v'_{0x} < 0$ by Eq.(25). This result means that if the ball is not released at the desired release time due to some errors, the rolling of the ball affects the release direction of the ball toward the target as shown in Fig.9. As a result robust control of the ball is achieved.

IV. EXPERIMENTS

A. System Configuration

The arm is a wire-drive manipulator (Barrett Technology Inc.). The kinematics of the manipulator is shown in Fig.10 (a). The manipulator has 4-DOF consisting of alternately revolution and bending motion. High-speed movement with maximum velocity of the end-effector of 6 [m/s] and maximum acceleration of 58 [m/s^2] is achieved.

The hand consists of three fingers and a wrist. It has 10-DOF in total. A small harmonic drive gear and a high-power mini actuator are fitted in each finger link [6]. The design of this actuator is based on the new concept that maximum power output, rather than rated power output, should be improved. The hand can close its joints at 180 [deg] per 0.1 [s]. Its maximum velocity is 300 [rpm], and the maximum output is 12 [N].

Figure 10 (b) shows the hand-arm system.

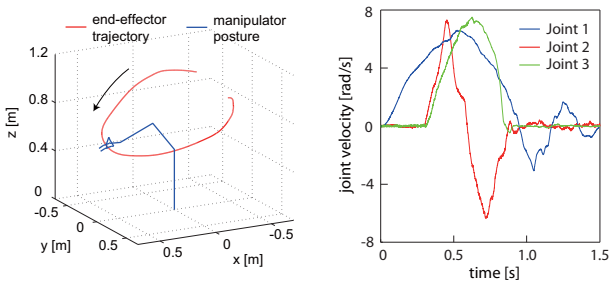

(a) Three dimensional trajectory (b) Joint velocity

Fig. 11. Experimental data of manipulator motion

B. Experimental Setting

The manipulator threw a urethane ball with radius 5 [cm] towards the target from 3 [m] distance. The target is a net with radius 10 [cm]. The dynamics of the swing model is transformed to the one corresponding to the arm shown in Fig.10 (a) due to the difference between mechanisms. In addition we adopted a gravity-compensated PD controller so as to enable accurate control of high-speed movement. Because the swing motion is generated so that Eq.(5) is satisfied, this simple controller plays an equivalent role as well as following the computed torque method;

$$\begin{aligned}\boldsymbol{\tau} &= \boldsymbol{g}(\boldsymbol{q}_d) + K_p\Delta\boldsymbol{q} + K_v\Delta\dot{\boldsymbol{q}} \\ &\simeq M\ddot{\boldsymbol{q}}_d + \boldsymbol{h}(\boldsymbol{q}_d, \dot{\boldsymbol{q}}_d) + \boldsymbol{g}(\boldsymbol{q}_d) + K_p\Delta\boldsymbol{q} + K_v\Delta\dot{\boldsymbol{q}}\ .\end{aligned} \tag{26}$$

C. Experimental Result

Figure 11 (a) shows the trajectory of the end-effector. It turns out that the motion in the z-axis direction oscillates around the height of the elbow. This is caused by the exp-type function. The time response of joint velocities is shown in Fig.11 (b). It turns out that both joint-1 and joint-3 correspond to a sin-type mode while joint-2 corresponds to an exp-type mode. The figure also indicates that accurate control on fast swing motion is achieved even by the simple controller except the overshoot of joint-1.

In Fig.12 and Fig.13, the change in contact state and the trajectory of a thrown ball are shown as a continuous sequence of pictures taken at intervals of 100 [ms] and 66 [ms] respectively. It turns out that grasping state with three fingers is switched to release state with two fingers, and then the ball is thrown toward the target.

The success rate was about 40 %. Failure was caused mainly by uncertainty in initial calibration of the grasping state and deviation from the contact model due to the elastic element of the ball. Accordingly, a tactile or force feedback control would improve the success rate. These experimental results are shown as a movie on the web site [7].

V. CONCLUSIONS

In this paper we presented a strategy for high-speed swing motion based on the kinetic chain approach. In addition, we analyzed the contact model for ball control. From this analysis, robust control of release direction was proposed.

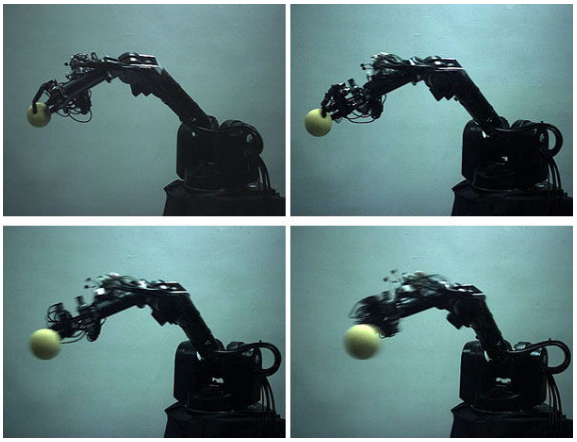

Fig. 12. Serial photographs of the change in contact state

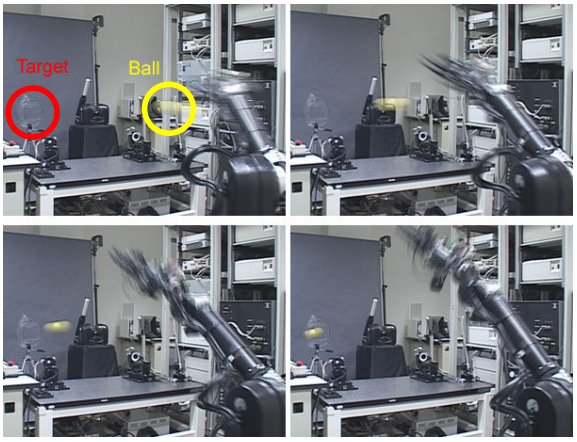

Fig. 13. Serial photographs of a ball thrown toward a target

As a result, the ball control in high-speed throwing motion was achieved using the hand-arm system.

Our future work will concentrate on a detailed robustness evaluation of ball control, and an adoption of tactile or force feedback control. Moreover we plan to control other high-speed dexterous manipulations with hand-arm coordination.

REFERENCES

[1] N. Furukawa, A. Namiki, T. Senoo and M. Ishikawa, *Dynamic Regrasping Using a High-speed Multifingered Hand and a High-speed Vision System*, Proc. of IEEE Int. Conf. on Robotics and Automation, pp.181-187, 2006.

[2] T. Senoo, A. Namiki and M. Ishikawa, *Ball Control in High-speed Batting Motion using Hybrid Trajectory Generator*, Proc. of IEEE Int. Conf. on Robotics and Automation, pp.1762-1767, 2006.

[3] S.L. Werner, *Biomechanics of the elbow during baseball pitching*, Journal of Orthop. Sports Phys. Ther, vol.17, No.6, pp.274-278, 1993.

[4] C.A. Putnam, *Sequential motions of body segments in striking and throwing skills*, J. of Biomech., pp.125-135, 1993.

[5] Y. Mochiduki and T. Matsuo and S. Inokuchi and K. Omura, *Dynamics analysis for the effect of centrifugal and coriolis forces in swing a bat*, Int. symp. on Biomechanics in Sports, pp.393-396, 1993.

[6] A. Namiki and Y. Imai and M. Ishikawa and M. Kaneko, *Development of a High-speed Multifingered Hand System and Its Application to Catching*, IEEE/RSJ Proc. of Int. Conf. on Intelligent Robots and Systems, pp.2666-2671, 2003.

[7] http://www.k2.t.u-tokyo.ac.jp/fusion/HighspeedThrowing/